

MSc Computational Neuroscience, Cognition and AI Research Project

Investigating the impact of traumatic brain injuries on brain connectivity changes for Alzheimer's disease using probabilistic tractography

Tom Aldridge
University of Nottingham
16th September 2022

Abstract

Traumatic brain injuries have significant lasting effects both in the short and long term, leading to death, disability, and neurodegeneration. In this report we investigate the links between traumatic brain injury and Alzheimer's disease (AD) through analysis of white matter integrity in Vietnam War veterans, finding changes in key brain pathways responsible for memory, learning, attention and motor skills. Diffusion weighted imaging (DWI) volumes, taken from the ADNI-DOD database, have probabilistic tractography performed on them to estimate tracts between defined regions. A tract-specific anisotropy (TSA) metric, which measures individual diffusion profiles, is then computed for each subject and regressed against subject-specific factors to find relationships between diffusion changes and injury specifics. We find that the severity of brain injury, along with experiencing altered mental state and being hospitalised, result in the largest negative brain connectivity changes between the locus coeruleus (LC), anterior cingulate cortex (ACC) and posterior cingulate gyrus (PCG). These results suggest that brain injuries have significant effects on structural connectivity, which may lead to cognitive decline and AD. However, war veterans are a small minority, and these results may not be indicative of the general populous.



**University of
Nottingham**
UK | CHINA | MALAYSIA

Contents

1	Introduction	3
2	Method	4
2.1	Data Exploration	4
2.2	ROI Definition	5
2.3	Processing	6
3	Results	8
4	Discussion	12
References		14
A	Anderson-Darling Test	18

List of Tables

1	Classification of TBI severity	5
---	--	---

List of Figures

1	Data exploration plots	5
2	Simplified tract determination procedure	8
3	Renders of tract determination	9
4	TSA distributions and heatmap renderings of TSA	10
5	Circular t-statistic plots	11
6	Scatter and violin plots for significant tracts	12

List of Abbreviations

ACC	Anterior Cingulate Cortex
AD	Alzheimer's Disease
ADNI	Alzheimer's Disease Neuroimaging Initiative
DMN	Default Mode Network
DTI	Diffusion Tensor Image
DWI	Diffusion Weighted Imaging

FA	Fractional Anisotropy
LC	Locus Coeruleus
NE	Norepinephrine
PCG	Posterior Cingulate Gyrus
PTSD	Post-Traumatic Stress Disorder
ROI	Region of Interest
TBI	Traumatic Brain Injury
TSA	Tract-Specific Anisotropy

1 Introduction

Traumatic brain injury (TBI) remains the leading cause of death and disability between the ages of 1 and 44 (Thurman, Alverson, Dunn, Guerrero, & Snieszek, 1999), with the global incidence of TBI estimated to be between 64 and 74 million individuals per year (Dewan et al., 2018). The highest rates of TBI occur from road traffic collisions, although head injuries from sports such as boxing and racing, work place accidents and falls also contribute. Following TBI, patients are often left with long-term physical, behavioural and emotional ramifications (Millis et al., 2001). The high human and social impact of these injuries places great importance on understanding the consequences of TBI. One such consequence is Alzheimer's disease (AD); many studies have been undertaken to investigate the relationship between AD and previous TBI, with multiple literature reviews confirming that AD can be a sequela of previous head injury (Fleminger, Oliver, Lovestone, Rabe-Hesketh, & Giora, 2003; Dams-O'Connor, Guetta, Hahn-Ketter, & Fedor, 2016). Notably, it has been revealed that amyloid- β ($A\beta$) plaques, a key indicator of AD, are found in up to 30% of patients who die acutely of TBI. Whilst concentrations of these plaques are typically found in elderly patients, post-TBI $A\beta$ plaque formation has been observed in all age groups, including children, just hours after injury (Johnson, Stewart, & Smith, 2010; Roberts et al., 1994). The primary form of the $A\beta$ protein found in these cases has been confirmed to be $A\beta_{42}$ (DeKosky et al., 2007; Gentleman et al., 1997), the same peptide that is found deposited on cortical areas of AD patients (Findeis, 2007).

Despite the focus on $A\beta$ deposition in the grey matter of the brain, evidence has shown that there is a relationship between AD and changes in the structure of white matter (Kao, Chou, Chen, & Yang, 2019; de Leeuw, Barkhof, & Scheltens, 2004). These abnormalities in white matter have been known to be responsible for the degradation of motor skills and coordination (Caeyenberghs et al., 2011; Zhai et al., 2020), key clinical indicators for the presentation of AD. Furthermore, the anomalies in white matter integrity and atrophy of brain mass in patients after TBI bears remarkable resemblance to abnormalities found in early AD patients (Fakhran, Yaeger, & Alhilali, 2013; Shively, Scher, Perl, & Diaz-Arrastia, 2012), suggesting similar neurodegeneration mechanisms. The study of these structural changes to white matter may be key to identifying the underlying process and risk profiles of TBI patients later developing AD.

Neuroimaging techniques such as diffusion-weighted imaging (DWI) can be used to estimate integrity of white matter *in vivo* through modelling diffusion of water molecules across sections of the brain across many differently orientated scans (Reid, Camilleri, Hoffstaedter, & Eickhoff, 2022). Diffusion occurs along myelinated axons due to their lipid-based, hydrophobic coating. If white matter, composed of axons, is structurally compromised due to either demyelination of axons or axonal loss, then the degree of anisotropy of diffusion will be decreased. A value of 0 for fractional anisotropy (FA) (Pierpaoli, Jezzard, Basser, Barnett, & Di Chiro, 1996) indicates uniform diffusion, whilst 1 indicates diffusion exclusively in the principal direction. This allows a map of diffusion pathways to be built up across the brain, indicating the positioning and orientation of axonal connections, as well as the integrity of these tracts. More specifically, streamlines are generated through starting at a set of seed voxels and sampling the most likely direction for each voxel from a posterior probability distribution of diffusion orientations, known as probabilistic tractography. Specific pathways between areas of grey matter can be investigated through the creation of a tract specific anisotropy (TSA) metric, which contains the likelihood of a tract existing between two areas, as well as the probable orientation (Reid et al., 2022). Different networks of regions of interest (ROI), such as the default mode network (DMN) or LCNET (Reid et al, in preparation. See section 2.2), which focuses on the locus coeruleus, an early pathological marker for AD (Braak & Del Tredici, 2012), can be specified and used to investigate key structural relationships. This imaging and analysis method is key for the discovery and visualisation of abnormalities in white matter.

This research aims to identify key areas and pathways of degradation across localised regions and the whole brain that may contribute to the onset of AD and cognitive decline in patients who have suffered previous TBI using DWI and TSA. Veterans of war, the focus of this study, have a high proportion of TBI and so confirming AD pathology following TBI, specifically in the locus coeruleus, may help for early diagnosis systems for AD and other dementias as well as for enhanced, targeted care for victims of TBI. Factors that may affect the progression of AD following TBI, such as time since injury, duration of amnesia, brain fog and unconsciousness will be investigated through elastic net regression.

2 Method

The data used to produce this study was sourced from the ADNI-DOD database (*Alzheimer’s Disease Neuroimaging Initiative*, 2004). The ADNI project was designed to “find more sensitive and accurate biomarkers for the early detection and tracking of AD” (from <https://adni.loni.usc.edu/about/>), through collecting and analysing brain scans, cognitive surveys and medical examinations. Studies using the ADNI dataset have already made key advancements in the field of AD, including identifying 10 genes thought to be responsible for AD (Saykin et al., 2010; Zhang et al., 2019), finding patterns of $A\beta$ deposition on cortical areas (Grothe & Teipel, 2015) and the existence of AD pathology in patients without memory loss complaints (Dubois et al., 2016). ADNI-DOD is an extension of these studies sponsored by the US Department of Defence, investigating the effects of TBI and PTSD on AD for veterans of the Vietnam War. All images taken in the ADNI-DOD study were performed at 3T using Siemens scanners, with 2mm isotropic voxels for $b = 0$ and 1000 s/mm^2 weighted volumes. The study consists of 315 patients (312 male, 2 female, 1 unknown) aged 60-80 years old. Metadata files containing the results of the aforementioned examinations were made available alongside brain scans from modalities including MRI, PET, fMRI, and the focus of our study, DWI. Before probabilistic tract spectography and other analysis could be performed, subjects had to be split into their classifications based on the severity of their TBI: severe, moderate, mild or control, i.e. no TBI. The method for this procedure will be explored in section 2.1.

2.1 Data Exploration

Metadata analysis was performed on a local Jupyter Notebook running Python 3.10.4 using *pandas*. Many patients received multiple scans throughout the course of the ADNI-DOD study. In this study we exclusively consider the first (or only) visit for each patient, removing the requirement to consider multiple longitudinal visits. Furthermore, the TSA method developed by Reid et al. (Reid et al., 2022) requires an axial DTI image, which not all patients received. A full list of patients who received axial DTI scans was downloaded from the ADNI-DOD database and all patients not on this list (48) were discarded from the study, leaving 264 valid subjects remaining. Of these 264 subjects, 170 subjects reported brain injuries for a total of 296 brain injury events. Subjects were then categorised depending on the severity of brain injury according to the guidelines set out in “Definition Of MTBI From The VA/DOD Clinical Practice Guideline For Management Of Concussion/Mild Traumatic Brain Injury”, Appendix C Table A-1 (O’Neil et al., 2013a), as replicated in Table 1. If subjects met criteria from different severity levels, the highest level achieved was assigned. A category of ”Insignificant” was also created for subjects who reported at least one count of TBI that did not meet the severity criteria as in Table 1. These subjects will not be included in the study due to the uncertainty regarding the extent of their injury. Patients who reported zero brain injuries (94) will be used as the control group to compare against. We note that this study specifically excludes patients with confirmed AD as an exclusion criteria.

A number of subjects reported receiving multiple brain injuries. These subjects are classified by their

Criteria	Mild	Moderate	Severe
Loss of consciousness	0-30 min	>30 min and <24 hrs	>24 hrs
Alteration of consciousness/mental state	Up to 24 hrs	>24 hours	
Post-traumatic amnesia	0 - 1 day	>1 and <7 days	>7 days

Table 1: Classification of TBI severity according to the Veteran’s Association/Department of Defence. Recreated from (O’Neil et al., 2013a). Meeting any of the criteria in a particular severity level designates the patient as such. If a patient meets the criteria of more than one category of severity, the higher severity level is assigned. If a patient has received multiple TBI of different severity, the highest severity achieved is assigned.

highest severity brain injury, and are also added to a list to investigate the impact of multiple brain injuries on AD. After removing duplicate entries and insignificant injuries from the data, 123 subjects remain; 41 with mild TBI, 37 with moderate TBI and 45 with severe TBI. These subjects are added to lists that are then used to procure data from the ADNI-DOD database, as well as for later steps in processing, as described in section 2.3. Despite evidence suggesting that pathological markers of AD develop shortly after TBI (Johnson et al., 2010), it is also important to consider the length of time since the injury occurred or age at injury, due to the correlation between age at injury and severity of TBI outcomes (Johnson & Stewart, 2015). To calculate time since injury, for each injured patient the difference was taken between the date of the injury and the date the scan was taken. The mean patient experienced this injury at 22.54 years of age and has been carrying it for 46.59 years more. In figure 1, we visualise the distribution of these ages and times since injury for each severity classification. A 3-sample Anderson-Darling test was performed on these different groups, verifying that at no significance level do the distributions of the ages of injury differ for different severities. This ensures that our results are not skewed by a particular severity of injury occurring at a significantly different age than others. This result can be seen in Appendix A.

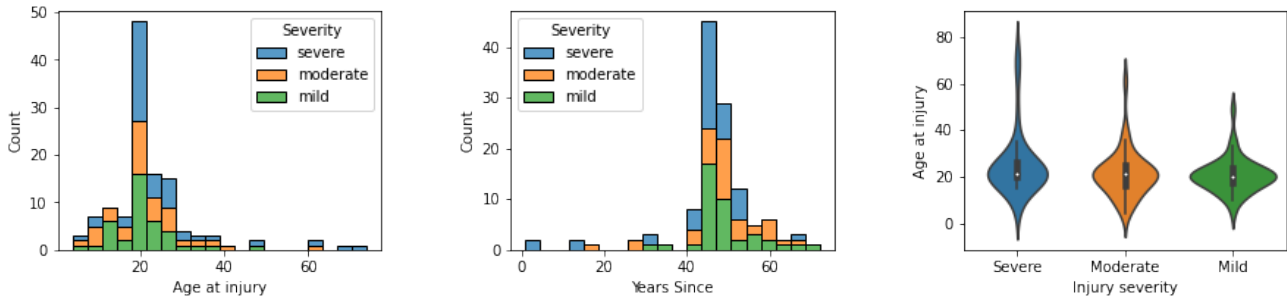


Figure 1: *Left:* Age at which injury occurred for each severity level. The average age of injury, 22.54, is very close to the average age of death of a Vietnam War soldier, 23.11 (*Vietnam War Facts, Stats and Myths*, n.d.). *Middle:* Years since injury occurred. The vast majority of subjects have been living with their injury for over 40 years, giving ample time for progression of disease indicators. *Right:* Violin plot showing distribution of ages at time of injury. We confirm that there is no significant difference in the distribution of ages at time of injury for different severity levels through a 3-sample Anderson-Darling test.

2.2 ROI Definition

ROIs are areas in the brain that we are interested in investigating the structural changes between following brain injuries. In this paper, we use the unpublished ROI network developed by Reid et al, called LCNET (Reid et al, in preparation). This network consists of 11 regions, from 3 cortical areas. The anterior cin-

gulate cortex (ACC) is split into 4 ROIs: dorsal left, dorsal right, ventral left and ventral right, where left and right refer to opposite hemispheres of the brain. These are referred to as **ACC1_left**, **ACC1_right** (dorsal), **ACC2_left** and **ACC2_right** (ventral). The anterior cingulate cortex provides connections between the thalamus and the ventral striatum, and is known to be responsible for motivated behaviour (Bonelli & Cummings, 2007), including attention allocation, decision making and impulse control. Disruptions to the circuitry in this region will cause degradation of these functions, and are also responsible for the presentation of the most common neuropsychiatric symptom of AD, apathy (Kim et al., 2011; Nobis & Husain, 2018). The next 6 regions are defined from the posterior cingulate gyrus (PCG), called **PCG1_left**, **PCG1_right**, **PCG2_left**, **PCG2_right**, **PCG3_left** and **PCG3_right**. This region is part of the limbic system and is connected to the parahippocampal gyrus, associated with memory and learning, as well as other regions that modulate emotion and awareness (Rolls, 2019). Studies have found the PCG to be affected early on in the progression of AD (Scheff et al., 2015), to the extent where it is considered one of the most vulnerable regions for AD-related decline (Lee et al., 2020).

The last region consists of the locus coeruleus (LC), located in the pons of the brain stem. The LC has widely distributed projections across the cortex (Aston-Jones & Cohen, 2005), and is the primary producer of the neuromodulator norepinephrine (NE). NE, through tonic activation, modulates effects on arousal, memory, mood, attention and motor skills (Berridge & Waterhouse, 2003; O'Donnell, Zeppenfeld, McConnell, Pena, & Nedergaard, 2012). Multiple studies confirm that degeneration of the LC-NE system have major effects on the brain, including increased neuronal deterioration, progression of cognitive decline and memory impairment (Matchett, Grinberg, Theofilas, & Murray, 2021; Van Egroo, Koshmanova, Vandewalle, & Jacobs, 2022). The accumulation of A β proteins and neurofibrillary tangles have been observed in the LC up to 20 years before discernible cognitive effects (Van Egroo et al., 2019), and are an early hallmark of AD (Braak & Del Tredici, 2012). Moreover, the connections between the LC and ACC maintain wakefulness and attentiveness, with cooperation required as neither is sufficient to maintain vigilance alone (Gompf et al., 2010). Visualising changes in these vulnerable areas, including the connections between them, is key to further understanding the pathology and progression of AD.

To generate the areas of these ROIs, two methods were used. Reid et al. (Reid et al 2022, in preparation) used pupil dilation related to resting-state fMRI to produce the ROIs for the ACC and PCG. This consists of scanning 50 subjects at resting state with a fixation cross for 5 minutes. The pupil diameter is convolved with a response function to compare to the fMRI. The temporal derivative of pupil diameter is computed and regressed against the fMRI signal to produce a statistical map (Yellin, Berkovich-Ohana, & Malach, 2015). This map is then used to generate the ROIs using a watershed algorithm in MATLAB. The LC ROI was obtained from (Keren, Lozar, Harris, Morgan, & Eckert, 2009). The authors method involved using a neuromelanin-sensitive turbo-spin echo MRI protocol on 44 adults aged between 19 and 79, taking two standard deviations of the result as the final ROI.

2.3 Processing

Before any meaningful analysis can be performed, multiple steps of pre-processing are required, including format conversion, Bayesian Estimation of Diffusion Parameters Obtained using Sampling Techniques (BedpostX) (Hernández et al., 2013) and probabilistic tractography (ProbtrackX) (Behrens et al., n.d.; Hernandez-Fernandez et al., 2019). The following section will discuss the steps required and the methods used in order to perform these processing steps. The computations described in this paper were performed using the University of Nottingham's Augusta HPC service, which provides a High Performance Computing service to the University's research community. See <https://www.nottingham.ac.uk/it-services/research/hpc/> for more details.

Data downloaded from the ADNI-DOD database is in the DICOM (Digital Imaging and Communi-

cations in Medicine) format, which is widely used across radiology, cardiology and radiotherapy devices (*DICOM*, n.d.). The format is known for being highly detailed and descriptive. However, as each DICOM file encodes a single 2D slice, across the multiple scans required to acquire an axial DTI image there may be hundreds or thousands of separate files (Li, Morgan, Ashburner, Smith, & Rorden, 2016). For a typical subject in our dataset there are 2714 files, totalling around 400MB of data per subject before any processing takes place. Alternatively, NIfTI (Neuroimaging Informatics Technology Initiative) provides a neuroimaging-specific format that is simpler and easier to manage, takes up less storage space and removes subject metadata that may be identifiable (*Neuroimaging Informatics Technology Initiative*, 2011). However, a conversion step is required to move between the two. A multi-platform conversion tool called `dcm2niix` (Li et al., 2016) provides a fast way to convert subjects to the NIfTI format. A custom script is used for batch processing on the University of Nottingham Augusta High Performance Computing (HPC) cluster. This script runs through each subject in the specified list and runs the conversion program on them, specifying output names and directories, as well as compressing the output. The resulting output are 4 files for a total of around 96MB, a ~75% decrease in file size.

NIfTI format images can then be fed into the image processing pipeline. These processes are run on the GPU of the Augusta HPC for increased parallel processing speed and are split into 3 parts. Each step utilises software from the Oxford Centre for Functional Magnetic Resonance Imaging of the Brain's (FMRIB) Diffusion Toolbox (FDT) (Woolrich et al., 2009). The first step, 'preproc', performs three functions: first, distortions caused by subject movement and eddy currents are corrected for. Non-brain areas such as the skull and other tissue are then removed from the image, known as brain extraction. Finally, a diffusion tensor model is fit at each voxel in the image. The next step in the processing pipeline performs BedpostX on each subject, which "runs Markov Chain Monte Carlo sampling to build up distributions on diffusion parameters at each voxel" (from [https://web.mit.edu/fsl_v5.0.10/fsl/doc/wiki/FDT\(2f\)UserGuide.html#BEDPOSTX](https://web.mit.edu/fsl_v5.0.10/fsl/doc/wiki/FDT(2f)UserGuide.html#BEDPOSTX)). This creates the necessary files to later run probabilistic tractography. The final stage, 'postproc', cleans up the file structures and moves directories when required and finally performs linear transforms, non-linear warps and inverse non-linear warps on the image files. These transforms are required to ensure that anatomical brain structures are represented in the same locations in different images, known as registration (Ou, Akbari, Bilello, Da, & Davatzikos, 2014).

After these processing steps have taken place, probabilistic tractography can be performed using FDT's `probtrackx2`. Starting from seeds initialised from the ROIs specified, tract orientation distributions obtained from the BedpostX step at each voxel are sampled from, followed, and terminated if any stopping criteria are met (i.e. the path has entered a region specified by the termination mask, the path has looped back on itself or the angle the path is required to take is too steep to be plausible). This builds up a distribution of probabilities of streamlines connecting brain regions. This data can then be used to determine tracts connecting brain areas of interest. It is important to note that throughout these processes 20 subjects, of varying severity level, had to be removed due to errors and incompatibilities during processing.

Tract determination begins by computing bidirectional average streamline probabilities between each pair of ROIs across all subjects. The distances between tracts are then calculated in both directions. "Core" tracts are then estimated by using the centre point of the voxel with the highest average streamline count passing through it as the first vertex of the path. This is repeated across the length of the tract, building the average streamline path between ROIs in both directions. An uncertainty field is expanded around this path and multiplied by the streamline probabilities to generate a bidirectional tract estimate. The tract-specific anisotropy (TSA) value for each subject, which shows how strongly an individual's diffusion profile lie along the average tract orientation, is calculated by first computing the average streamline orientation across all subjects for each tract, and then regressing this against amount of diffusion found in each subject. This shows the variability of tracts across subjects.

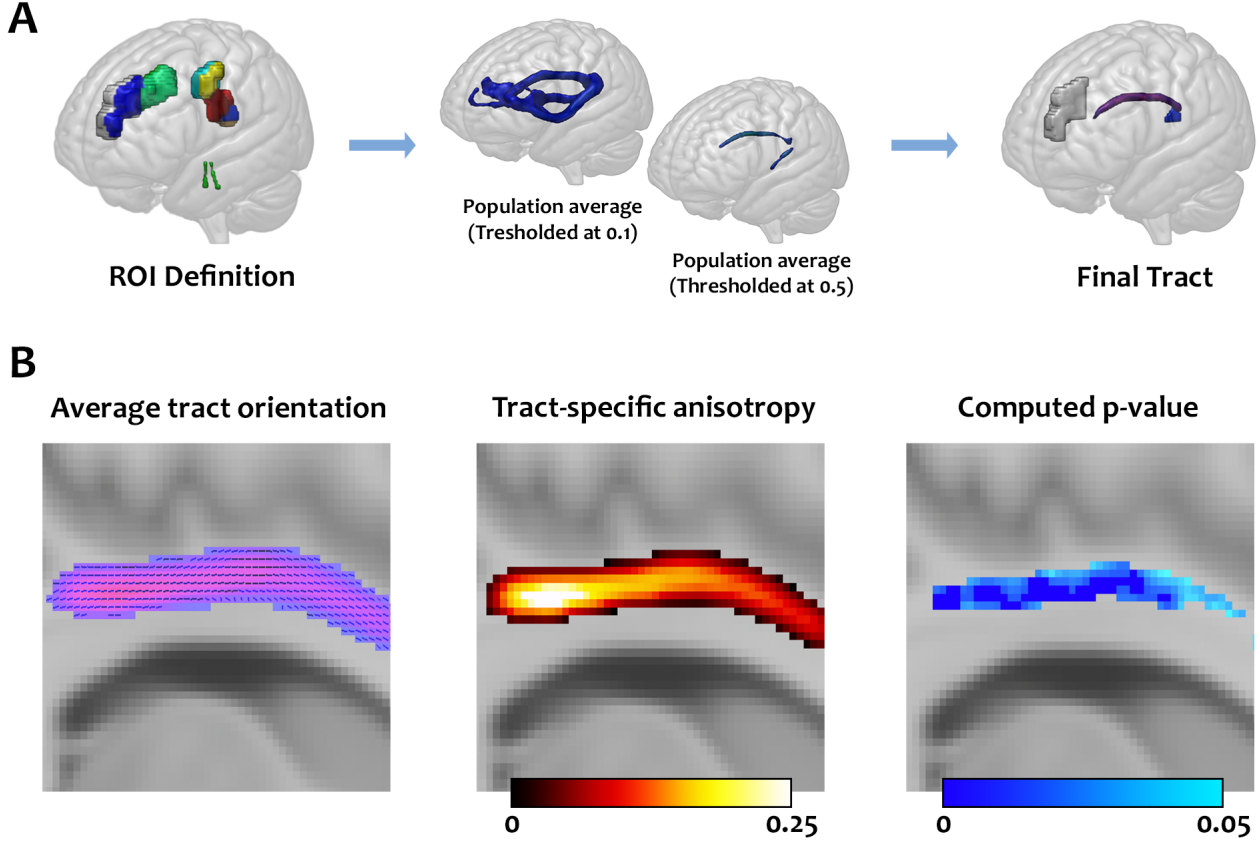


Figure 2: Simplified tract determination procedure. *Top:* ROIs are used to seed streamlines that build up connectivity probability distributions. These can be thresholded to only show voxels that have a high probability of a tract passing through them. The final tract is built up of the average streamline path multiplied by an gaussian uncertainty field. *Bottom:* Average tract orientations are used to build up average diffusion profiles, called tract-specific anisotropy. These are regressed against subject-specific factors to find p-values for the significance of the factor's effect on tract degradation. These values are for a GLM performed on TSA values vs severity, and are exemplar rather than conveying results.

Statistical analysis is performed on the computed TSA values to determine the significance of subject-specific factors, such as severity of TBI or age at injury, on individual diffusion profiles. The factors used were derived from the subject metadata files and were specified in csv format. For every voxel in a tract, a linear regression of the form $\mathbf{Y} = \mathbf{X}\beta$ was performed, where \mathbf{Y} are the TSA values, \mathbf{X} are the factors and β are the coefficients to fit. T-statistics are computed from the fitted coefficients, which are then used to determine p-values for each voxel. Using `fdr_tsby` from the `statsmodels` Python library, the p-values are corrected for family-wise error by using a false discovery rate (FDR) threshold of 0.05. The resulting output maps the values determined at each stage onto the coordinates of the voxels, allowing the output to be visualised as in figure 2B.

3 Results

Out of 55 bidirectional tracts attempted, 52 (94.5%) tracts were found between 11 different brain areas. Failed tracts occurred at ACC1L - PCG3R, PCG2R - PCG3R and ACC1R - PCG2L, visualised in figure 3c. We note that 2 of these tracts are contralateral, while the other connects 2 very close brain regions.

Reid et al. state that these failed tracts may occur due to thresholding of the bidirectional averages causing a break in the continuous path between ROIs, or if a single core tract fails to emerge. It is important to note that this does not mean that the tract does not exist, but instead there is insufficient diffusion evidence to determine the exact location and path of the tract (Reid et al., 2022). Distributions of TSA values for each tract thresholded at $P_{ab_tract} > 0.5$, averaged across all subjects, are displayed in figure 4a. The majority of tracts have normally distributed TSA values, with a very slight positive skew. Some tracts showed very little variance in their values, such as PCG3L - PCG3R, while others such as PCG1L - PCG2R show high kurtosis. The mode TSA value across all subjects and tracts was 0.13. Figure 4b shows TSA values for each voxel for 2 tracts. The maximal TSA value tends to be found in the centre of each tract.

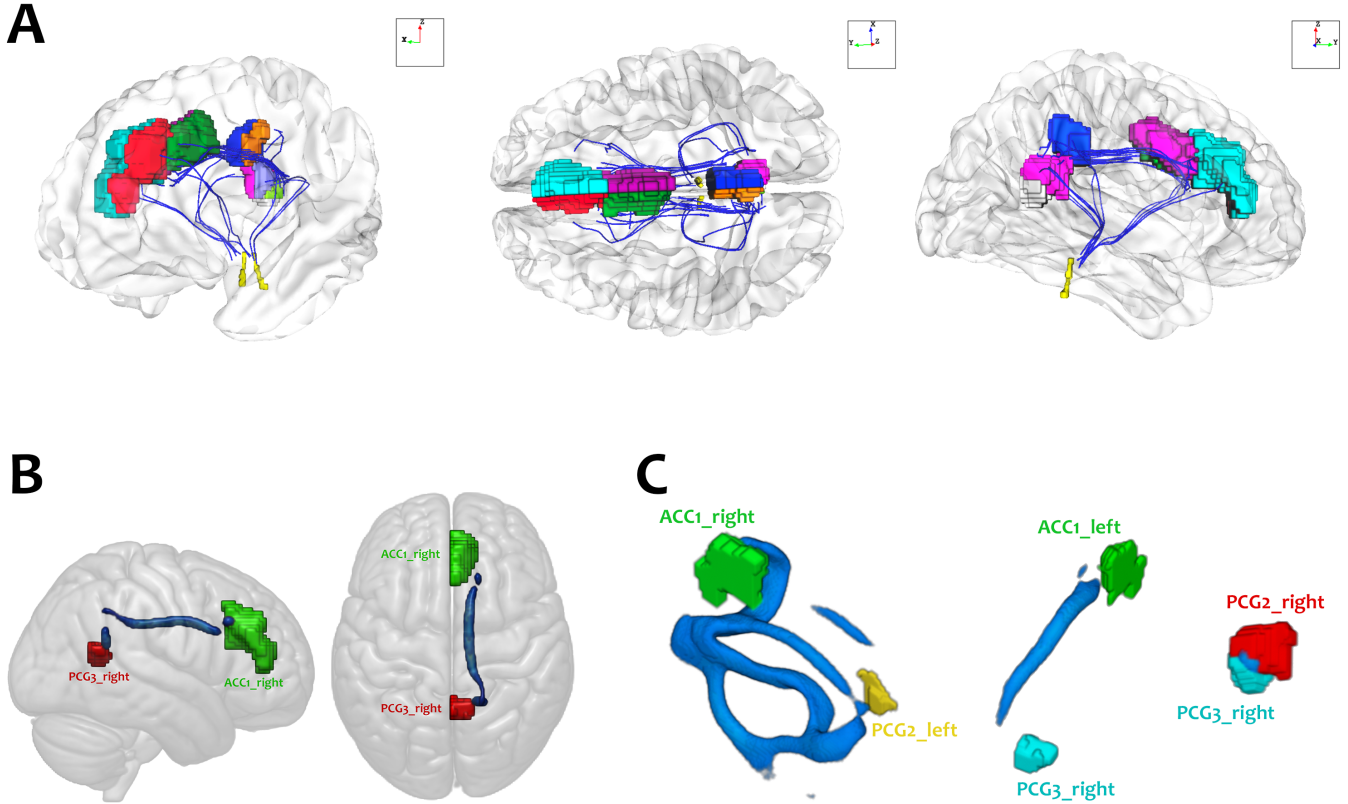


Figure 3: Renders from MRIcroGL and ModelGUI of tract determination. **A:** Estimated core trajectory (blue lines) of all accepted tracts between all ROIs (varying colours). Calculated from connecting voxels with maximum streamline count. **B:** Final tract between PCG3_right and ACC1_right, thresholded at 0.2. **C:** Average streamline probabilities thresholded at 0.2 for all ROI pairs that failed to produce a final tract. The tract between ACC1_right and PCG2_left failed to determine a final tract due to multiple paths existing at the threshold.

Statistical analysis was then performed on the 52 final tracts for the following factors that may affect the integrity of white matter following TBI: severity classification, age at injury, time since injury, as well as the factors that built up the severity classification, including amnesia duration, altered mental state duration (hereby called *brain fog*) and loss of consciousness duration. Figure 5 shows circular representations of summed significant t-statistics for a selection of these factors between each tract. We find that the severity of TBI is the most dramatic indicator of reduced diffusion profiles in the brain, with 43/52 (82.7%) tracts showing negative effects. The strongest effect is seen in the tract between ACC1L and PCG2R, with an R^2 value of 0.147. Strong negative effects are also seen for patients that reported

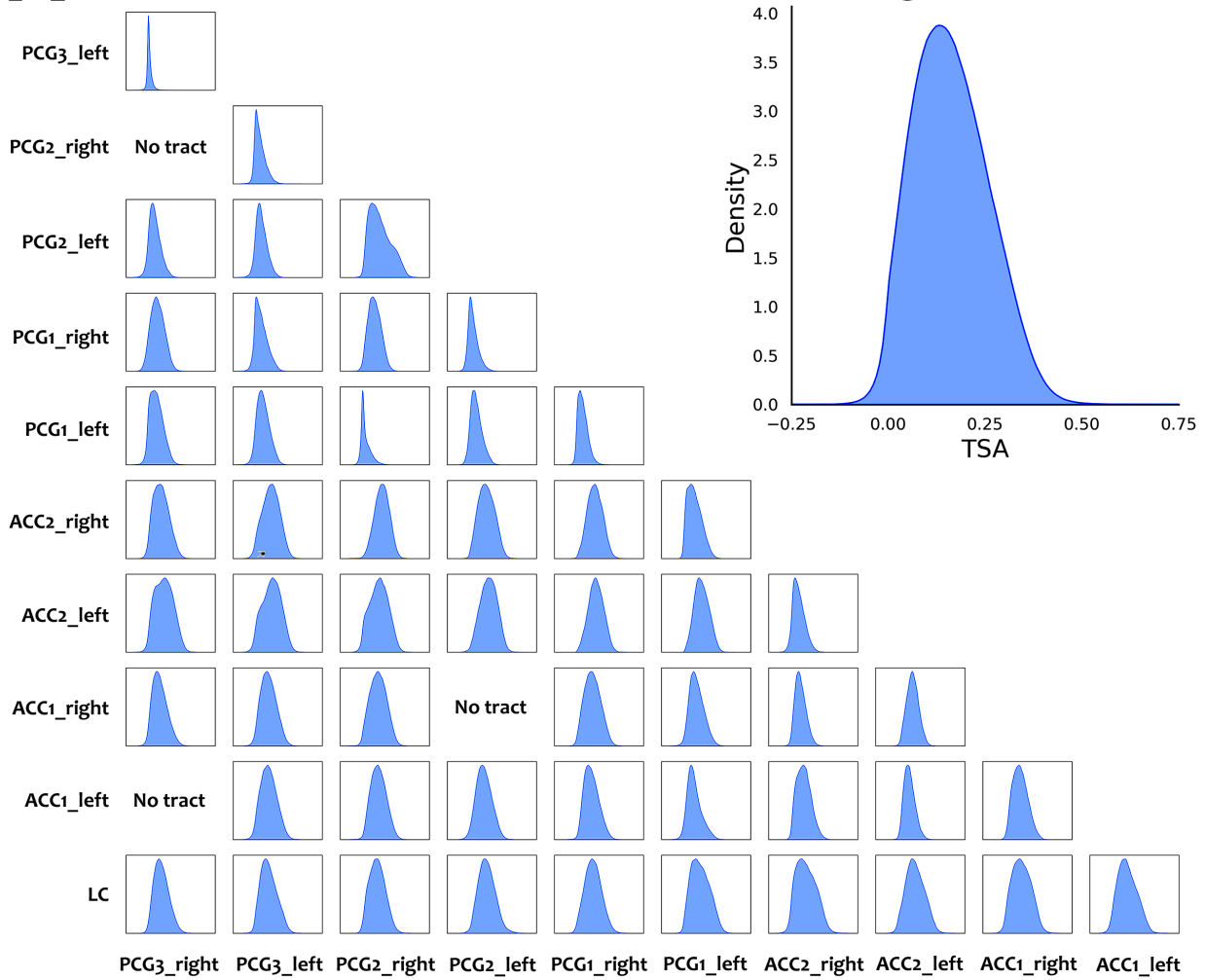
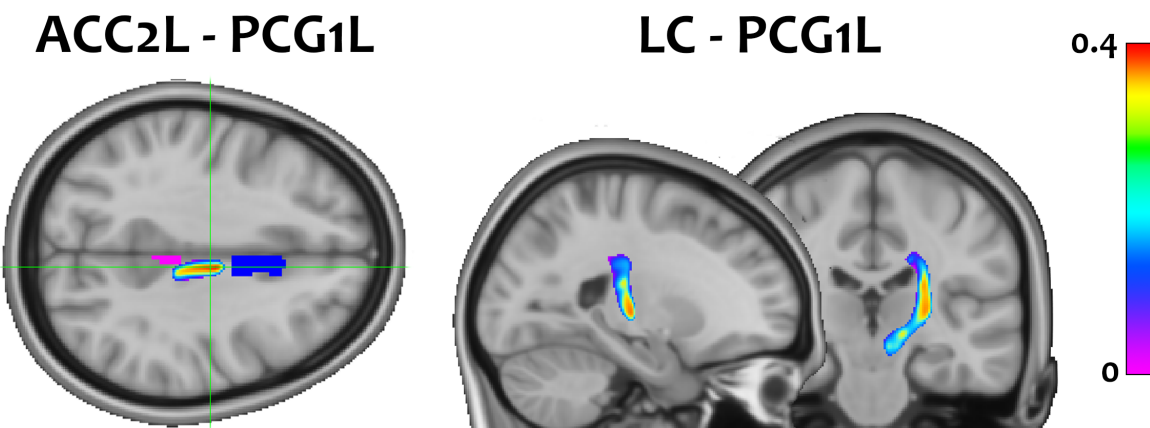
A**B**

Figure 4: **A:** Distribution of computed TSA values averaged across all participants for all pairs of ROIs. TSA values cannot be computed for tracts that have no final bidirectional tract estimate. The inset graph shows the distribution of TSA values across all tracts and subjects. **B:** Heatmap renderings of TSA values for 2 tracts overlaid on the standard MNI152 T1-weighted template.

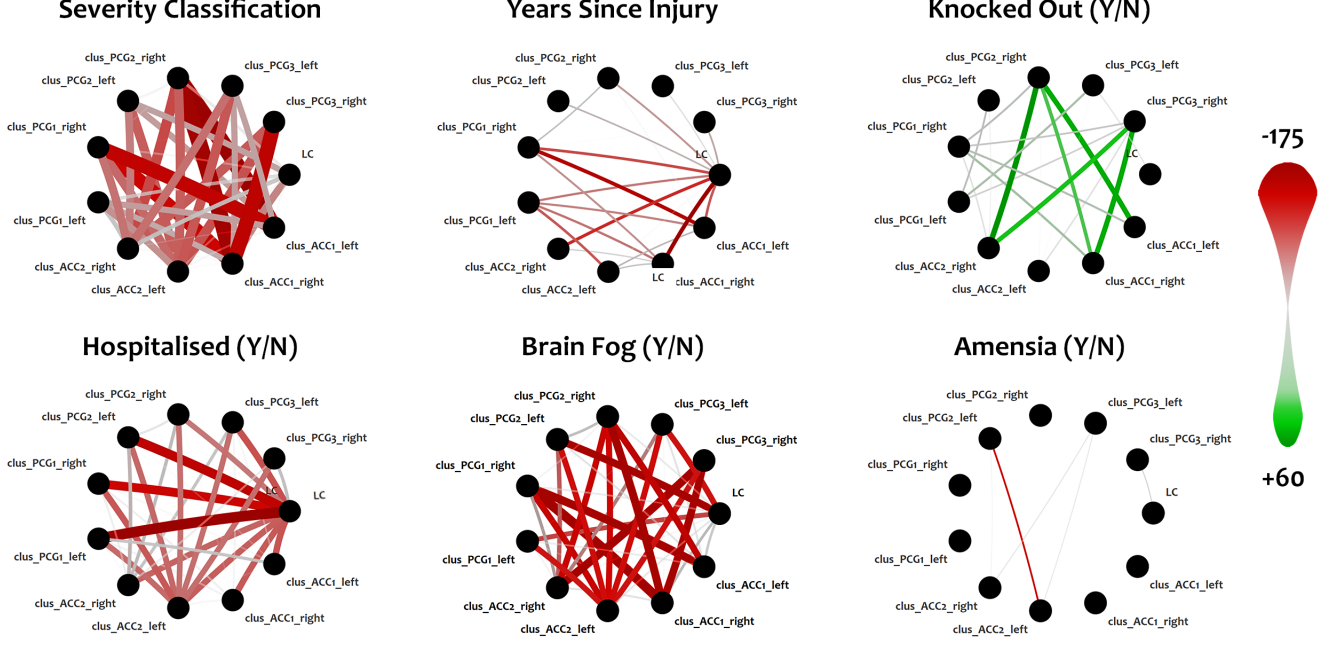


Figure 5: Summed t-statistics for a selection of regressed factors. T-statistics are summed separately for positive and negative clusters. Thickness and saturation represents strength of change of TSA due to factor, colour represents positive (green) or negative (red) change. Maximum changes in TSA found in higher severity injury patients, while small positive changes appear to occur after being knocked unconscious.

being hospitalised following their brain injury, with 36/62 (69.2%) tracts reporting significant change, particularly between LC and PCG1L. The extent to which this factor can be considered an indicator will be explored in section 4. Age at injury and years since injury occurred resulted in remarkably similar changes in TSA, reporting 27 and 24 tracts with significant effect respectively. In both cases, the LC - ACC1R tract showed the most negative effect. However, as these are calculated from each other (years since = date of scan - year of injury), meaningful relationships are hard to uncover.

Considering the factors that constitute the severity classification, experiencing brain fog following injury appears have to significant negative effects on tract specific anisotropy, with 37/52 (71.2%) of tracts across our ROIs showing high degradation. The most severe of these tend to be between the ACC and the PCC. The damage is not localised to any ROI, with at least 2 significant negative tracts being found between every ROI, as seen in figure 5. ACC2L experienced the most widespread connectivity damage, with 6 very significant tracts, whilst the tract ACC1R - PCG1R had the most severe effect. The duration of this brain fog had no significant effect on TSA. We also find negative effects for patients who have experienced amnesia in 6 brain tracts. The tracts connecting PCG3 (left and right) to the LC, ACC2 and PCG1, as well as the tracts from ACC2 (left and right) to PCG2L, all show degradation in diffusion profiles following an injury that causes amnesia. The duration of amnesia experienced has considerable effects on the tracts between the LC and ACC2L and the LC and ACC1L. Interconnecting tracts between the PCC also experience higher degradation following extended amnesic periods. Contrastingly, being knocked out showed positive effects for 30 tracts (57.7%), with the most severe effect seen for tract ACC2R - PCG3R. Relative to the other indicators in this report, these effects are comparatively weak, but are nonetheless still present. However, the validity of these results may be questioned upon inspection of the violin plots shown in figure 6. For the most significant positive tract ACC2R - PCG3R, the TSA values for knocked out patients are characterised by longer tails than the not knocked out group. The mean is overall higher for the prior group, but the distributions are arguably similar. However, for the unconscious group, the

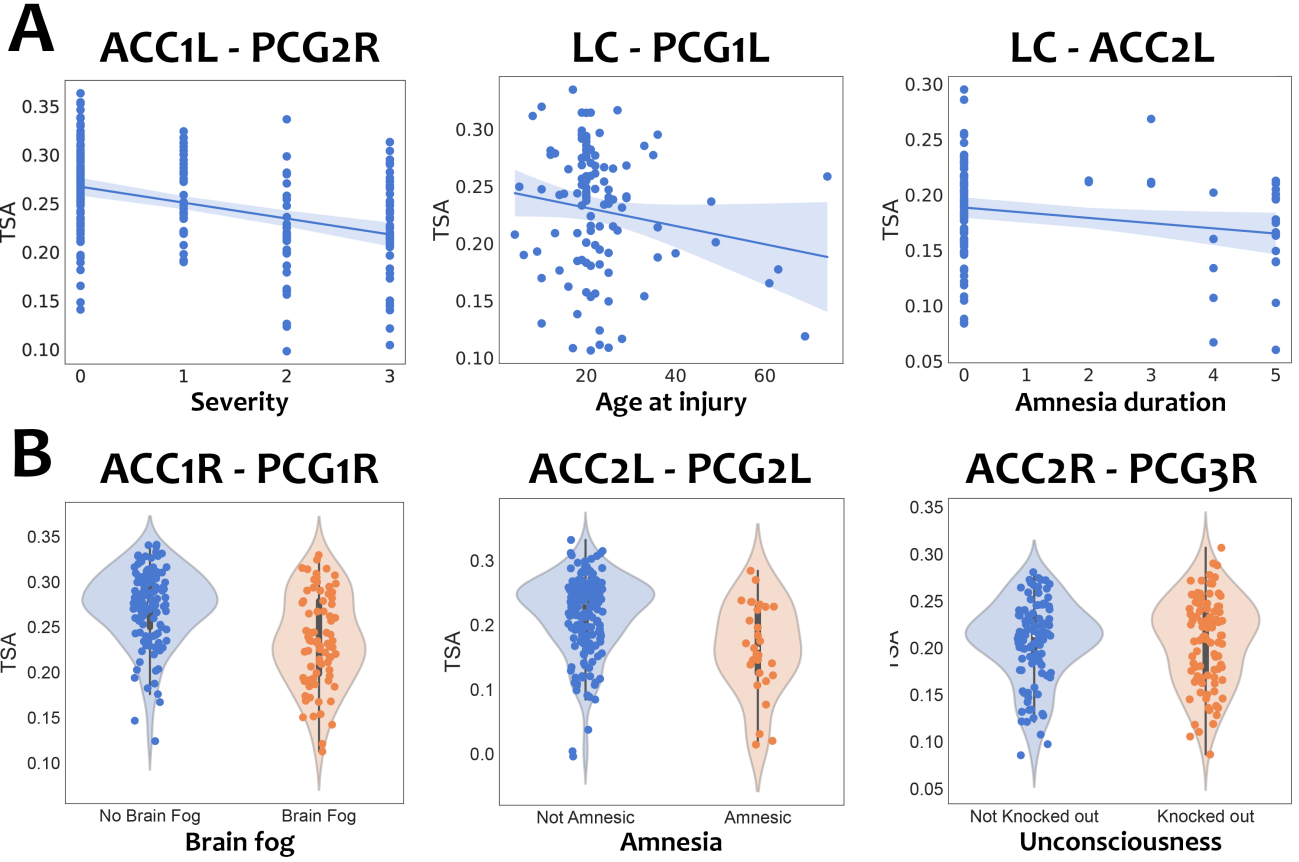


Figure 6: Scatter and violin plots for a selection of the most significant tracts. **A:** *Left:* Severity ranges from 0, no injury, to 3, most severe. Strong negative correlation is seen for increasing severity classification. *Middle:* War veterans mostly experienced their injuries at around the same age, skewing the dataset. The wide 95% confidence interval suggests uncertainty in the regression. *Right:* Increased duration of amnesia post TBI predicts lower TSA values. **B:** *Left and middle:* Experiencing brain fog and amnesia after brain injury widens the range of TSA values computed, with lower overall mean value. *Right:* The data suggests that mean TSA values after being knocked unconscious increase. The spread of both maximum and minimum non-outlying values is greater after unconsciousness.

duration of unconsciousness does have negative effects on TSA: 4 interconnecting tracts within the PCC show decreased diffusion as the duration of unconsciousness increases.

4 Discussion

This paper has identified key tracts through DWI between key brain areas with high risk of deterioration following TBI leading to the progression of AD-like symptoms. The diffusion profiles built up through computational analysis of these tracts have been regressed against to find significant relationships between severity of injury, experience of altered mental state and unconsciousness, amongst other factors. We now use these diffusion profiles to relate to white matter integrity in the brain and discuss the relationship between decreased fractional anisotropy and the pathology of AD. AD-risk is found to be associated with white matter integrity (Gold, Johnson, Powell, & Smith, 2012a), so it is important to analyse causes of degradation of white matter. Overall, we have found evidence to suggest that TSA decreases following TBI in principal pathways between brain areas responsible for memory, awareness, decision making and motor control. This corroborates studies performed on the pathology of AD using similar methods,

which found similar degeneration of FA in subjects experiencing AD (Hall et al., 2021; Teipel et al., 2014; Timpe, Rowe, Matsui, Magnotta, & Denburg, 2011). The severity of brain injury, as classified as in (O’Neil et al., 2013b), has the most significant effect on TSA, followed by experiencing altered mental state, then whether the subject was hospitalised for their brain injury, as also found in (Delano-Wood et al., 2015; Kraus et al., 2007). Degradation is also related to age at/time since injury, duration of amnesic period and, interestingly, inversely related to whether the subject was made unconscious by their injury. This inverse relationship disagrees with the previously cited findings and suggests anomalous behaviour.

Diffusion profiles of tracts to and from the LC were often the most deteriorated, across many regressed factors. This suggests that LC connectivity is greatly influenced by brain injury. Valko et al. concur, finding that after brain injury noradrenergic neuron counts decreased by 29% in the LC (Valko et al., 2016). When combined with the knowledge of how NE dysfunction contributes to cognitive decline and AD (David et al., 2022; Gannon et al., 2015), and the importance of the connections between the LC and the ACC for functions such as attention (Gompf et al., 2010), it is obvious that this system is at great risk and focus should be placed on limiting and treating degradation of LC white matter.

Despite these results, it is important to consider the limitations of this work, starting with the data itself. The metadata collected that was used to regress against TSA values was acquired through multiple interviews and surveys with the participants. Whilst patients with above-threshold mild cognitive impairment scores or other dementias were excluded by design, a large proportion of the cohort still reported memory complaints and scored highly on the Telephone Interview for Cognitive Status (TICS) test. As such, the validity of their answers is called into question, specifically their ability to recall factors such as the length of their amnesic period, brain fog, and loss of consciousness. As these were the key constituents of the severity classification, it is appropriate to treat these results with some uncertainty. Furthermore, we found hospitalisation of the subject to be a marker for decreased white matter integrity following injury. However, being hospitalised often depends on the audience of the injury, especially if the subject is unconscious. There may have been cases where subjects with very minor injury have been taken as a precaution, whilst more severe injuries could be ignored. As the subject cohort were exclusively Vietnam War veterans, it is also possible that they were subjected to alternative mental or physical stresses, or may have been experiencing PTSD, which has been found to increase risk of cognitive decline or AD (Desmarais et al., 2020; Yaffe et al., 2010). As such, they may not be representative of the general populous.

Studies have also found white matter vulnerabilities related to AD in other regions of the brain, including the parahippocampus, temporoparietal junction and the anterior insula (Gold, Johnson, Powell, & Smith, 2012b; Liebe et al., n.d.). As such, an expansion of the brain network used may be beneficial to further understanding of the extent of AD pathology following TBI. Furthermore, the method used relies on many parameters used for thresholding, outlier removal and `probtrackx` arguments. These values were chosen heuristically in order to limit tracts in reasonable ways, however these values can be tweaked to bias the results. See (Reid et al., 2022) for more intricate critique of the method used.

This report provides evidence towards the hypothesis that TBI causes degradation of white matter tracts in the brain related to memory, cognition, and attention, however it is unclear how strong this relationship is to the progression of AD. Further investigation is required using expanded subject cohorts, including wider age groups and non-war veterans, as well as the regression of other factors that introduce AD risk such as PTSD and depression. This, combined with existing research into tau pathology and A β deposition, would allow for a wider view of factors affecting white matter degeneration leading to decreased diffusion and structural connectivity in AD patients, with the aim of identifying demographics that are at significant risk of AD.

References

- Alzheimer's Disease Neuroimaging Initiative.* (2004). Department of Defence.
- Aston-Jones, G., & Cohen, J. D. (2005). AN INTEGRATIVE THEORY OF LOCUS COERULEUS-NOREPINEPHRINE FUNCTION: Adaptive Gain and Optimal Performance. *Annual Review of Neuroscience*, 28(1), 403–450. doi: 10.1146/annurev.neuro.28.061604.135709
- Behrens, T. E. J., Woolrich, M. W., Jenkinson, M., Johansen-berg, H., Nunes, R. G., Matthews, P. M., ... Smith, S. M. (n.d.). *Characterization and Propagation of Uncertainty in Diffusion Weighted MR images*.
- Berridge, C. W., & Waterhouse, B. D. (2003, April). The locus coeruleus–noradrenergic system: Modulation of behavioral state and state-dependent cognitive processes. *Brain Research Reviews*, 42(1), 33–84. doi: 10.1016/S0165-0173(03)00143-7
- Bonelli, R. M., & Cummings, J. L. (2007). Frontal-subcortical circuitry and behavior. *Dialogues in Clinical Neuroscience*, 9(2), 141–151.
- Braak, H., & Del Tredici, K. (2012, December). Where, when, and in what form does sporadic Alzheimer's disease begin? *Current Opinion in Neurology*, 25(6), 708–714. doi: 10.1097/WCO.0b013e32835a3432
- Caeyenberghs, K., Leemans, A., Geurts, M., Linden, C. V., Smits-Engelsman, B. C. M., Sunaert, S., & Swinnen, S. P. (2011, July). Correlations Between White Matter Integrity and Motor Function in Traumatic Brain Injury Patients. *Neurorehabilitation and Neural Repair*, 25(6), 492–502. doi: 10.1177/1545968310394870
- Dams-O'Connor, K., Guetta, G., Hahn-Ketter, A. E., & Fedor, A. (2016, October). Traumatic brain injury as a risk factor for Alzheimer's disease: Current knowledge and future directions. *Neurodegenerative Disease Management*, 6(5), 417–429. doi: 10.2217/nmt-2016-0017
- David, M. C. B., Giovane, M. D., Liu, K. Y., Gostick, B., Rowe, J. B., Oboh, I., ... Malhotra, P. A. (2022, October). Cognitive and neuropsychiatric effects of noradrenergic treatment in Alzheimer's disease: Systematic review and meta-analysis. *Journal of Neurology, Neurosurgery & Psychiatry*, 93(10), 1080–1090. doi: 10.1136/jnnp-2022-329136
- DeKosky, S. T., Abrahamson, E. E., Ciallella, J. R., Paljug, W. R., Wisniewski, S. R., Clark, R. S. B., & Ikonomovic, M. D. (2007, April). Association of Increased Cortical Soluble A β 42 Levels With Diffuse Plaques After Severe Brain Injury in Humans. *Archives of Neurology*, 64(4), 541–544. doi: 10.1001/archneur.64.4.541
- Delano-Wood, L., Bangen, K. J., Sorg, S. F., Clark, A. L., Schiehser, D. M., Luc, N., ... Bigler, E. D. (2015, September). Brainstem white matter integrity is related to loss of consciousness and postconcussive symptomatology in veterans with chronic mild to moderate traumatic brain injury. *Brain Imaging and Behavior*, 9(3), 500–512. doi: 10.1007/s11682-015-9432-2
- de Leeuw, F.-E., Barkhof, F., & Scheltens, P. (2004, January). White matter lesions and hippocampal atrophy in Alzheimer's disease. *Neurology*, 62(2), 310–312. doi: 10.1212/01.WNL.0000103289.03648.AD
- Desmarais, P., Weidman, D., Waslef, A., Bruneau, M.-A., Friedland, J., Bajcarowicz, P., ... Nguyen, Q. D. (2020, January). The Interplay Between Post-traumatic Stress Disorder and Dementia: A Systematic Review. *The American Journal of Geriatric Psychiatry*, 28(1), 48–60. doi: 10.1016/j.jagp.2019.08.006
- Dewan, M. C., Rattani, A., Gupta, S., Baticulon, R. E., Hung, Y.-C., Punchak, M., ... Park, K. B. (2018, April). Estimating the global incidence of traumatic brain injury. *Journal of Neurosurgery*, 130(4), 1080–1097. doi: 10.3171/2017.10.JNS17352
- DICOM. (n.d.). <https://www.dicomstandard.org>.
- Dubois, B., Hampel, H., Feldman, H. H., Scheltens, P., Aisen, P., Andrieu, S., ... Jack, C. R. (2016, March). Preclinical Alzheimer's disease: Definition, natural history, and diagnostic cri-

- teria. *Alzheimer's & dementia : the journal of the Alzheimer's Association*, 12(3), 292–323. doi: 10.1016/j.jalz.2016.02.002
- Fakhraian, S., Yaeger, K., & Alhilali, L. (2013, October). Symptomatic White Matter Changes in Mild Traumatic Brain Injury Resemble Pathologic Features of Early Alzheimer Dementia. *Radiology*, 269(1), 249–257. doi: 10.1148/radiol.13122343
- Findeis, M. A. (2007, November). The role of amyloid β peptide 42 in Alzheimer's disease. *Pharmacology & Therapeutics*, 116(2), 266–286. doi: 10.1016/j.pharmthera.2007.06.006
- Fleminger, S., Oliver, D. L., Lovestone, S., Rabe-Hesketh, S., & Giora, A. (2003, July). Head injury as a risk factor for Alzheimer's disease: The evidence 10 years on; a partial replication. *Journal of Neurology, Neurosurgery & Psychiatry*, 74(7), 857–862. doi: 10.1136/jnnp.74.7.857
- Gannon, M., Che, P., Chen, Y., Jiao, K., Roberson, E. D., & Wang, Q. (2015, June). Noradrenergic dysfunction in Alzheimer's disease. *Frontiers in Neuroscience*, 9, 220. doi: 10.3389/fnins.2015.00220
- Gentleman, S. M., Greenberg, B. D., Savage, M. J., Noori, M., Newman, S. J., Roberts, G. W., ... Graham, D. I. (1997, April). A B42 is the predominant form of amyloid β -protein in the brains of short-term survivors of head injury. *NeuroReport*, 8(6), 1519–1522.
- Gold, B. T., Johnson, N. F., Powell, D. K., & Smith, C. D. (2012a, March). White matter integrity and vulnerability to Alzheimer's disease: Preliminary findings and future directions. *Biochimica Et Biophysica Acta*, 1822(3), 416–422. doi: 10.1016/j.bbadi.2011.07.009
- Gold, B. T., Johnson, N. F., Powell, D. K., & Smith, C. D. (2012b, March). White matter integrity and vulnerability to Alzheimer's disease: Preliminary findings and future directions. *Biochimica et Biophysica Acta*, 1822(3), 416–422. doi: 10.1016/j.bbadi.2011.07.009
- Gompf, H. S., Mathai, C., Fuller, P. M., Wood, D. A., Pedersen, N. P., Saper, C. B., & Lu, J. (2010, October). Locus Ceruleus and Anterior Cingulate Cortex Sustain Wakefulness in a Novel Environment. *Journal of Neuroscience*, 30(43), 14543–14551. doi: 10.1523/JNEUROSCI.3037-10.2010
- Grothe, M. J., & Teipel, S. J. (2015, October). Spatial patterns of atrophy, hypometabolism, and amyloid deposition in Alzheimer's disease correspond to dissociable functional brain networks. *Human Brain Mapping*, 37(1), 35–53. doi: 10.1002/hbm.23018
- Hall, J. R., Johnson, L. A., Zhang, F., Petersen, M., Toga, A. W., Shi, Y., ... Study, f. t. H. (2021). Using Fractional Anisotropy Imaging to Detect Mild Cognitive Impairment and Alzheimer's Disease among Mexican Americans and Non-Hispanic Whites: A HABLE Study. *Dementia and Geriatric Cognitive Disorders*, 50(3), 266–273. doi: 10.1159/000518102
- Hernández, M., Guerrero, G. D., Cecilia, J. M., García, J. M., Inuggi, A., Jbabdi, S., ... Sotiroopoulos, S. N. (2013). Accelerating fibre orientation estimation from diffusion weighted magnetic resonance imaging using GPUs. *PLoS One*, 8(4), e61892. doi: 10.1371/journal.pone.0061892
- Hernandez-Fernandez, M., Reguly, I., Jbabdi, S., Giles, M., Smith, S., & Sotiroopoulos, S. N. (2019, March). Using GPUs to accelerate computational diffusion MRI: From microstructure estimation to tractography and connectomes. *NeuroImage*, 188, 598–615. doi: 10.1016/j.neuroimage.2018.12.015
- Johnson, V. E., & Stewart, W. (2015, March). Age at injury influences dementia risk after traumatic brain injury. *Nature reviews. Neurology*, 11(3), 128–130. doi: 10.1038/nrneurol.2014.241
- Johnson, V. E., Stewart, W., & Smith, D. H. (2010, May). Traumatic brain injury and amyloid- β pathology: A link to Alzheimer's disease? *Nature reviews. Neuroscience*, 11(5), 361–370. doi: 10.1038/nrn2808
- Kao, Y.-H., Chou, M.-C., Chen, C.-H., & Yang, Y.-H. (2019, February). White Matter Changes in Patients with Alzheimer's Disease and Associated Factors. *Journal of Clinical Medicine*, 8(2), 167. doi: 10.3390/jcm8020167
- Keren, N. I., Lozar, C. T., Harris, K. C., Morgan, P. S., & Eckert, M. A. (2009, October). In vivo mapping of the human locus coeruleus. *NeuroImage*, 47(4), 1261–1267. doi: 10.1016/j.neuroimage.2009.06.012
- Kim, J. W., Lee, D. Y., Choo, I. H., Seo, E. H., Kim, S. G., Park, S. Y., & Woo, J. I. (2011, July).

- Microstructural alteration of the anterior cingulum is associated with apathy in Alzheimer disease. *The American Journal of Geriatric Psychiatry: Official Journal of the American Association for Geriatric Psychiatry*, 19(7), 644–653. doi: 10.1097/JGP.0b013e31820dcc73
- Kraus, M. F., Susmaras, T., Caughlin, B. P., Walker, C. J., Sweeney, J. A., & Little, D. M. (2007, October). White matter integrity and cognition in chronic traumatic brain injury: A diffusion tensor imaging study. *Brain*, 130(10), 2508–2519. doi: 10.1093/brain/awm216
- Lee, P.-L., Chou, K.-H., Chung, C.-P., Lai, T.-H., Zhou, J. H., Wang, P.-N., & Lin, C.-P. (2020). Posterior Cingulate Cortex Network Predicts Alzheimer's Disease Progression. *Frontiers in Aging Neuroscience*, 12.
- Li, X., Morgan, P. S., Ashburner, J., Smith, J., & Rorden, C. (2016, May). The first step for neuroimaging data analysis: DICOM to NIfTI conversion. *Journal of Neuroscience Methods*, 264, 47–56. doi: 10.1016/j.jneumeth.2016.03.001
- Liebe, T., Dordevic, M., Kaufmann, J., Avetisyan, A., Skalej, M., & Müller, N. (n.d.). Investigation of the functional pathogenesis of mild cognitive impairment by localisation-based locus coeruleus resting-state fMRI. *Human Brain Mapping*, n/a(n/a). doi: 10.1002/hbm.26039
- Matchett, B. J., Grinberg, L. T., Theofilas, P., & Murray, M. E. (2021, May). The mechanistic link between selective vulnerability of the locus coeruleus and neurodegeneration in Alzheimer's disease. *Acta Neuropathologica*, 141(5), 631–650. doi: 10.1007/s00401-020-02248-1
- Millis, S. R., Rosenthal, M., Novack, T. A., Sherer, M., Nick, T. G., Kreutzer, J. S., ... Ricker, J. H. (2001, August). Long-Term Neuropsychological Outcome After Traumatic Brain Injury. *The Journal of Head Trauma Rehabilitation*, 16(4), 343–355.
- Neuroimaging Informatics Technology Initiative* [Document]. (2011). <https://nifti.nimh.nih.gov/background>.
- Nobis, L., & Husain, M. (2018, August). Apathy in Alzheimer's disease. *Current Opinion in Behavioral Sciences*, 22, 7–13. doi: 10.1016/j.cobeha.2017.12.007
- O'Donnell, J., Zeppenfeld, D., McConnell, E., Pena, S., & Nedergaard, M. (2012, November). Norepinephrine: A Neuromodulator That Boosts the Function of Multiple Cell Types to Optimize CNS Performance. *Neurochemical research*, 37(11), 2496–2512. doi: 10.1007/s11064-012-0818-x
- O'Neil, M. E., Carlson, K., Storzbach, D., Brenner, L., Freeman, M., Quiñones, A., ... Kansagara, D. (2013a). *Complications of Mild Traumatic Brain Injury in Veterans and Military Personnel: A Systematic Review*. Washington (DC): Department of Veterans Affairs (US).
- O'Neil, M. E., Carlson, K., Storzbach, D., Brenner, L., Freeman, M., Quiñones, A., ... Kansagara, D. (2013b, January). *Table A-1, Classification of TBI Severity* [Text]. <https://www.ncbi.nlm.nih.gov/books/NBK189784/table/appc.t1/>. Department of Veterans Affairs (US).
- Ou, Y., Akbari, H., Bilello, M., Da, X., & Davatzikos, C. (2014, October). Comparative Evaluation of Registration Algorithms in Different Brain Databases With Varying Difficulty: Results and Insights. *IEEE transactions on medical imaging*, 33(10), 2039–2065. doi: 10.1109/TMI.2014.2330355
- Pierpaoli, C., Jezzard, P., Bassar, P. J., Barnett, A., & Di Chiro, G. (1996, December). Diffusion tensor MR imaging of the human brain. *Radiology*, 201(3), 637–648. doi: 10.1148/radiology.201.3.8939209
- Reid, A. T., Camilleri, J. A., Hoffstaedter, F., & Eickhoff, S. B. (2022, December). Tract-specific statistics based on diffusion-weighted probabilistic tractography. *Communications Biology*, 5(1), 138. doi: 10.1038/s42003-022-03073-w
- Roberts, G. W., Gentleman, S. M., Lynch, A., Murray, L., Landon, M., & Graham, D. I. (1994, April). Beta amyloid protein deposition in the brain after severe head injury: Implications for the pathogenesis of Alzheimer's disease. *Journal of Neurology, Neurosurgery & Psychiatry*, 57(4), 419–425. doi: 10.1136/jnnp.57.4.419
- Rolls, E. T. (2019). The cingulate cortex and limbic systems for emotion, action, and memory. *Brain Structure & Function*, 224(9), 3001–3018. doi: 10.1007/s00429-019-01945-2

- Saykin, A. J., Shen, L., Foroud, T. M., Potkin, S. G., Swaminathan, S., Kim, S., ... Initiative, A. D. N. (2010). Alzheimer's Disease Neuroimaging Initiative biomarkers as quantitative phenotypes: Genetics core aims, progress, and plans. *Alzheimer's & Dementia*, 6(3), 265–273. doi: 10.1016/j.jalz.2010.03.013
- Scheff, S. W., Price, D. A., Ansari, M. A., Roberts, K. N., Schmitt, F. A., Ikonomovic, M. D., & Mufson, E. J. (2015). Synaptic Change in the Posterior Cingulate Gyrus in the Progression of Alzheimer's Disease. *Journal of Alzheimer's disease : JAD*, 43(3), 1073–1090. doi: 10.3233/JAD-141518
- Shively, S., Scher, A. I., Perl, D. P., & Diaz-Arrastia, R. (2012, October). Dementia Resulting From Traumatic Brain Injury. *Archives of neurology*, 69(10), 1245–1251. doi: 10.1001/archneurol.2011.3747
- Teipel, S. J., Grothe, M. J., Filippi, M., Fellgiebel, A., Dyrba, M., Frisoni, G. B., ... EDSD study group (2014). Fractional anisotropy changes in Alzheimer's disease depend on the underlying fiber tract architecture: A multiparametric DTI study using joint independent component analysis. *Journal of Alzheimer's disease: JAD*, 41(1), 69–83. doi: 10.3233/JAD-131829
- Thurman, D. J., Alverson, C., Dunn, K. A., Guerrero, J., & Snieszek, J. E. (1999, December). Traumatic Brain Injury in the United States: A Public Health Perspective. *The Journal of Head Trauma Rehabilitation*, 14(6), 602–615.
- Timpe, J. C., Rowe, K. C., Matsui, J., Magnotta, V. A., & Denburg, N. L. (2011). White matter integrity, as measured by diffusion tensor imaging, distinguishes between impaired and unimpaired older adult decision-makers: A preliminary investigation. *Journal of cognitive psychology (Hove, England)*, 23(6), 760–767. doi: 10.1080/20445911.2011.578065
- Valko, P. O., Gavrilov, Y. V., Yamamoto, M., Noaín, D., Reddy, H., Haybaeck, J., ... Scammell, T. E. (2016, June). Damage to Arousal-Promoting Brainstem Neurons with Traumatic Brain Injury. *Sleep*, 39(6), 1249–1252. doi: 10.5665/sleep.5844
- Van Egroo, M., Koshmanova, E., Vandewalle, G., & Jacobs, H. I. L. (2022, April). Importance of the locus coeruleus-norepinephrine system in sleep-wake regulation: Implications for aging and Alzheimer's disease. *Sleep Medicine Reviews*, 62, 101592. doi: 10.1016/j.smrv.2022.101592
- Van Egroo, M., Narbutas, J., Chylinski, D., Villar González, P., Maquet, P., Salmon, E., ... Vandewalle, G. (2019, April). Sleep-wake regulation and the hallmarks of the pathogenesis of Alzheimer's disease. *Sleep*, 42(4), zsz017. doi: 10.1093/sleep/zsz017
- Vietnam War Facts, Stats and Myths*. (n.d.). <https://www.uswings.com/about-us-wings/vietnam-war-facts/>.
- Woolrich, M. W., Jbabdi, S., Patenaude, B., Chappell, M., Makni, S., Behrens, T., ... Smith, S. M. (2009, March). Bayesian analysis of neuroimaging data in FSL. *NeuroImage*, 45(1, Supplement 1), S173-S186. doi: 10.1016/j.neuroimage.2008.10.055
- Yaffe, K., Vittinghoff, E., Lindquist, K., Barnes, D., Covinsky, K. E., Neylan, T., ... Marmar, C. (2010, June). Post-Traumatic Stress Disorder and Risk of Dementia among U.S. Veterans. *Archives of general psychiatry*, 67(6), 608–613. doi: 10.1001/archgenpsychiatry.2010.61
- Yellin, D., Berkovich-Ohana, A., & Malach, R. (2015, February). Coupling between pupil fluctuations and resting-state fMRI uncovers a slow build-up of antagonistic responses in the human cortex. *NeuroImage*, 106, 414–427. doi: 10.1016/j.neuroimage.2014.11.034
- Zhai, F., Liu, J., Su, N., Han, F., Zhou, L., Ni, J., ... Zhu, Y. (2020, October). Disrupted white matter integrity and network connectivity are related to poor motor performance. *Scientific Reports*, 10(1), 18369. doi: 10.1038/s41598-020-75617-1
- Zhang, D.-F., Fan, Y., Xu, M., Wang, G., Wang, D., Li, J., ... Yao, Y.-G. (2019, March). Complement C7 is a novel risk gene for Alzheimer's disease in Han Chinese. *National Science Review*, 6(2), 257–274. doi: 10.1093/nsr/nwy127

Appendix

A Anderson-Darling Test

The Anderson-Darling test was performed on the ages at which injury occurred for each different severity level, severe, moderate and mild. The test was performed in Python 3.10.4 using `stats.anderson_kamp()` from `scipy.stats` 1.7.3. The test returned a statistic of -0.20 with critical values [0.45, 1.94, 2.58, 3.42, 4.07] for significance levels [25%, 10%, 5%, 2.5%, 1%], meaning that the null hypothesis that the samples are drawn from the same distribution cannot be rejected at any significance level.